Development of a Novel Anti-CD44 Variant 7/8 Monoclonal Antibody C44Mab-34 for Multiple Applications against Oral Carcinomas

Hiroyuki Suzuki [*,#] , Kazuki Ozawa [#] , Tomohiro Tanaka , Mika K. Kaneko , Yukinari Kato [*]

Posted Date: 27 February 2023

doi: 10.20944/preprints202302.0437.v1

Keywords: CD44; CD44 variant 7/8; monoclonal antibody; flow cytometry; immunohistochemistry

Article

Development of a Novel Anti-CD44 Variant 7/8 Monoclonal Antibody C44Mab-34 for Multiple Applications against Oral Carcinomas

Hiroyuki Suzuki *,#, Kazuki Ozawa #, Tomohiro Tanaka, Mika K. Kaneko and Yukinari Kato *

Department of Antibody Drug Development, Tohoku University Graduate School of Medicine, 2-1 Seiryo-machi, Aoba-ku, Sendai 980-8575, Miyagi, Japan; ozawa.kazuki.s5@dc.tohoku.ac.jp (K.O); tomohiro.tanaka.b5@tohoku.ac.jp (T.T.); k.mika@med.tohoku.ac.jp (M.K.K.)

* Correspondence: hiroyuki.suzuki.b4@tohoku.ac.jp (H. S.); yukinari.kato.e6@tohoku.ac.jp (Y.K); Tel.: +81-29-853-3944 (H.S., Y.K.)

# contributed equally to this work

Abstract: Cluster of differentiation 44 (CD44) has been investigated as a cancer stem cell (CSC) marker, and plays critical roles in tumor malignant progression. The splicing variants are overexpressed in many carcinomas, especially squamous cell carcinomas, and play critical roles in the promotion of tumor metastasis, the acquisition of CSC properties, and resistance to treatments. Therefore, each CD44 variant (CD44v) function and distribution in carcinomas should be clarified for the establishment of novel tumor diagnosis and therapy. In this study, we immunized mice with a CD44 variant (CD44v3−10) ectodomain and established various anti-CD44 monoclonal antibodies (mAbs). One of the established clones (C44Mab-34; IgG_1, kappa) recognized a peptide which covers both variant 7 and 8-encoded region, indicating that C44Mab-34 is a specific mAb for CD44v7/8. Moreover, C44Mab-34 reacted with CD44v3–10-overexpressed Chinese hamster ovary-K1 (CHO) cells or oral squamous cell carcinoma (OSCC) cell line (HSC-3) by flow cytometry. The apparent K_D of C44Mab-34 for CHO/CD44v3–10 and HSC-3 was 1.4×10^{-9} M and 3.2×10^{-9} M, respectively. C44Mab-34 could detect CD44v3–10 in western blotting, and stained the formalin-fixed paraffin-embedded OSCC in immunohistochemistry. These results indicate that C44Mab-34 is useful for detecting CD44v7/8 in various applications, and expected for the application of OSCC diagnosis and therapy.

Keywords: CD44; CD44 variant 7/8; monoclonal antibody; flow cytometry; immunohistochemistry

1. Introduction

Head and neck cancers mainly arise from the oral cavity, pharynx, larynx, and nasal cavity. These tumors exhibit strong associations with smoking tobacco products, alcohol, and infection with human papillomavirus (HPV) types 16 and 18 [1]. The estimated new cases of oral cavity and pharynx in United States increased from 35,310 in 2008 to 54,540 in 2023, due to rising HPV-positive cases [2-4]. Mortality rates continue to increase for the oral cavity cancers associated with HPV-infection (cancers of the tongue, tonsil, and oropharynx), by about 2% per year in men and 1% per year in women [2].

Although many different histologies exist in head and neck cancers, head and neck squamous cell carcinoma (HNSCC) is the common type. The treatment options of HNSCC include surgery, chemo-radiation, molecular targeted therapy, immunotherapy, or a combination of these modalities [5]. Despite the development in cancer treatment, metastasis and drug resistance remain the main causes of deaths [6]. Although survival can be improved, the impairment due to surgery and the toxicities of treatments deteriorate the patients' quality of life. Thus, the 5-year survival rate remains stagnant at approximately 50% [1].

Cancer stem cells (CSC) play critical roles in tumor development through their important properties, including self-renewal, resistance to therapy, and tumor metastasis [7-9]. Studies have

 doi:10.20944/preprints202302.0437.v1

reported the importance of CSC in HNSCC development [10], and regulation by both intrinsic and extrinsic mechanisms in the tumor microenvironment [11]. Several cell surface receptors and intracellular proteins have been reported as applicable CSC markers in HNSCC [12,13]. Among them, cluster of differentiation 44 (CD44) is one of the important CSC markers in solid tumors, and first applied to study HNSCC-derived CSCs [14]. Notably, CD44-high CSCs from HNSCC tumors exhibited the properties of epithelial to mesenchymal transition, including elevated migration, invasiveness, and stemness [15]. Furthermore, CD44-high cells could form lung metastases in immunodeficient mice, in contrast to CD44-low, which failed to exhibit similar metastatic proliferation of cancer cells [16]. Therefore, specific monoclonal antibodies (mAbs) against CD44 are required for the isolation of CD44-high CSCs and the analysis of their properties in detail.

CD44 is a multifunctional transmembrane protein, which binds to extracellular matrix including hyaluronic acid (HA) [17]. Human CD44 has 19 exons, 10 of which are constant, or present, in all variants and makes up the standard form of CD44 (CD44s). The CD44 variants (CD44v) are produced by alternative splicing and consist of the 10 constant exons in any combination with the remaining nine variant exons [18]. The CD44 isoforms have both overlapping and unique roles. Both CD44s and CD44v (pan-CD44) possess HA-binding motifs that promote interaction with the microenvironment and facilitate activation of various signaling pathways [19].

Overexpression of CD44v has been observed in many types of carcinomas, and considered as a promising target for tumor diagnosis and therapy [20,21]. There is a growing number of evidence that CD44v plays important roles in the promotion of tumor metastasis, the acquisition of CSC properties [22], and the resistance to chemotherapy and radiotherapy [23,24]. Several variant exon-encoded regions have been reported to promote tumorigenesis through their interacting proteins. The v3-encoded region has heparan sulfate moieties, and can recruit to fibroblast growth factors (FGFs) and heparin-binding epidermal growth factor-like growth factor (HB-EGF). Thus, the v3-encoded region functions as a co-receptor of receptor tyrosine kinases [25]. Furthermore, the v6-encoded region was reported to be essential for the activation of c-MET through formation of ternary complex with HGF [26]. Moreover, the v8–10-encoded region mediates the oxidative stress resistance through regulation of intracellular redox states. [27]. Therefore, CD44v-specific mAbs are required not only for the understanding of each variant function but also for the CD44v-targeting tumor diagnosis and therapy. However, the function and distribution of the variant encoded region in tumors have not been fully understood.

Our group have developed the Cell-Based Immunization and Screening (CBIS) method and established a novel anti-pan-CD44 mAb, C$_{44}$Mab-5 (IgG$_1$, kappa) [28]. We also established another anti-pan-CD44 mAb, C$_{44}$Mab-46 (IgG$_1$, kappa) [29] using the immunization of CD44v3–10 ectodomain (CD44ec). We determined the epitopes of C$_{44}$Mab-5 and C$_{44}$Mab-46 in the standard exons (1 to 5)-encoding sequences [30-32]. We further showed that both C$_{44}$Mab-5 and C$_{44}$Mab-46 are available for flow cytometry, western blot, and immunohistochemistry in oral SCC (OSCC) [28] and esophageal SCC [29]. Furthermore, we have also investigated the antitumor effects using recombinant C$_{44}$Mab-5 in mouse xenograft models of oral OSCC [33]. We converted the mouse IgG$_1$ subclass antibody (C$_{44}$Mab-5) into an IgG$_{2a}$ subclass antibody (5-mG$_{2a}$), and further produced a defucosylated version (5-mG$_{2a}$-f) using FUT8-deficient ExpiCHO-S (BINDS-09) cells. The 5-mG$_{2a}$-f showed moderate *in vitro* ADCC and CDC activities against HSC-2 and SAS OSCC cell lines. Furthermore, the 5-mG$_{2a}$-f significantly reduced tumor growth in HSC-2 and SAS xenografts compared to control mouse IgG [33]. These results suggested that treatment with 5-mG$_{2a}$-f may represent a useful therapy for patients with CD44-expressing oral cancers. Here, we developed a novel anti-CD44v7/8 mAb, C$_{44}$Mab-34 (IgG$_1$, kappa), and examined its applications to flow cytometry, western blotting, and immunohistochemical analyses.

 doi:10.20944/preprints202302.0437.v1

2. Materials and Methods

2.1. Cell lines

CHO-K1, a glioblastoma cell line (LN229), and mouse multiple myeloma P3X63Ag8U.1 (P3U1) cell lines were obtained from the American Type Culture Collection (ATCC, Manassas, VA, USA). Human OSCC cell line, HSC-3 were obtained from the Japanese Collection of Research Bioresources (Osaka, Japan). CHO-K1 and P3U1 were cultured in Roswell Park Memorial Institute (RPMI)-1640 medium (Nacalai Tesque, Inc., Kyoto, Japan), supplemented with 100 U/mL penicillin, 100 µg/mL streptomycin, 0.25 µg/mL amphotericin B (Nacalai Tesque, Inc.), and 10% heat-inactivated fetal bovine serum (FBS; Thermo Fisher Scientific, Inc., Waltham, MA, USA).

LN229 and HSC-3 were cultured in Dulbecco's Modified Eagle Medium (DMEM) (Nacalai Tesque, Inc.), supplemented with 10% (*v*/*v*) FBS, 100 U/mL of penicillin (Nacalai Tesque, Inc.), 100 µg/mL streptomycin (Nacalai Tesque, Inc.), 0.25 µg/mL amphotericin B (Nacalai Tesque, Inc.). LN229/CD44ec was cultured in the presence of 0.5 mg/mL of G418 (Nacalai Tesque, Inc.).

All the cells were grown in a humidified incubator at 37°C with 5% CO_2.

2.2. Plasmid construction and establishment of stable transfectants

CD44v3–10 open reading frame (ORF) was obtained from the RIKEN BRC through the National Bio-Resource Project of the MEXT, Japan. CD44s cDNA was amplified using HotStar HiFidelity Polymerase Kit (Qiagen Inc., Hilden, Germany) using LN229 cDNA as a template. The CD44s and CD44v3–10 ORFs were subcloned into pCAG−Ble−ssPA16 vector possessing signal sequence and N−terminal PA16 tag (GLEGGVAMPGAEDDVV) [28,34-37], which is detected by NZ-1, which was originally developed as an anti-human podoplanin mAb [38-53].

CHO/CD44s and CHO/CD44v3−10 was established by transfecting the plasmids into CHO−K1 cells using a Neon transfection system (Thermo Fisher Scientific, Inc.). CD44ec−secreting LN229 (LN229/CD44ec) was established by transfecting pCAG−Neo/PA−CD44ec−RAP−MAP into LN229 cells using the Neon transfection system. The amino acid sequences of the tag system in this study were as follows: PA tag [43,47,51], 12 amino acids (GVAMPGAEDDVV); RAP tag [54,55], 12 amino acids (DMVNPGLEDRIE); and MAP tag [56,57], 12 amino acids (GDGMVPPGIEDK).

2.3. Purification of CD44ec

The purification of CD44ec from the culture supernatant of LN229/CD44ec was preformed using an anti-RAP tag mAb (clone PMab−2) and a RAP peptide (GDDMVNPGLEDRIE) [54,55]. The culture supernatant (5 L) was passed through 2 mL bed volume of PMab-2-Sepharose, and the process was repeated three times. After washing the beads with 100 mL of phosphate-buffered saline (PBS, Nacalai Tesque, Inc.), CD44ec was eluted with 0.1 mg/mL of a RAP peptide in a step-wise manner (2 mL × 10).

2.4. Hybridomas

The female BALB/c mice were purchased from CLEA Japan (Tokyo, Japan). All animal experiments were also conducted according to relevant guidelines and regulations to minimize animal suffering and distress in the laboratory. The Animal Care and Use Committee of Tohoku University (Permit number: 2019NiA-001) approved animal experiments. The immunization of CD44ec was performed as described previously [29].

The splenic cells were fused with P3U1 cells using polyethylene glycol 1500 (PEG1500; Roche Diagnostics, Indianapolis, IN, USA). The hybridomas were then grown in RPMI media supplemented with hypoxanthine, aminopterin, and thymidine (HAT) for selection (Thermo Fisher Scientific Inc.). The culture supernatants were screened for the ant-CD44ec antibody production using enzyme−linked immunosorbent assay (ELISA). The supernatants were further screened using CHO/CD44v3–10 and parental CHO-K1 cells by the flow cytometry-based high throughput screening using SA3800 Cell Analyzers (Sony Corp. Tokyo, Japan).

2.5. ELISA

Fifty-eight synthesized peptides, which cover the CD44v3–10 extracellular domain [30], were synthesized by Sigma-Aldrich Corp. (St. Louis, MO, USA) The peptides (1 μg/mL) and CD44ec were immobilized on Nunc Maxisorp 96-well immunoplates (Thermo Fisher Scientific Inc) for 30 min at 37°C. After washing with PBS containing 0.05% (*v*/*v*) Tween 20 (PBST; Nacalai Tesque, Inc.) using Microplate Washer, HydroSpeed (Tecan, Zürich, Switzerland), wells were blocked with 1% (*w*/*v*) bovine serum albumin (BSA; Nacalai Tesque, Inc.)-containing PBST for 30 min at 37°C. C44Mab-34 (10 μg/mL) were added to each well, and then incubated with peroxidase-conjugated anti-mouse immunoglobulins (1:2000 diluted; Agilent Technologies Inc., Santa Clara, CA, USA). Enzymatic reactions were performed using 1-Step Ultra TMB (Thermo Fisher Scientific Inc.). The optical density at 655 nm was mesured using an iMark microplate reader (Bio-Rad Laboratories, Inc., Berkeley, CA, USA).

2.6. Flow cytometry

CHO-K1, CHO/CD44v3–10, and HSC-3 were harvested using 0.25% trypsin and 1 mM ethylenediamine tetraacetic acid (EDTA; Nacalai Tesque, Inc.). The cells were treated with C44Mab-34, C44Mab-46, or blocking buffer (control) (0.1% BSA in PBS) for 30 min at 4°C. Then, the cells were treated with Alexa Fluor 488-conjugated anti-mouse IgG (1:2000; Cell Signaling Technology, Inc, Danvers, MA, USA) for 30 min at 4°C. Fluorescence data were collected using the SA3800 Cell Analyzer and analyzed using SA3800 software ver. 2.05 (Sony Corporation).

2.7. Determination of dissociation constant (K_D) via flow cytometry

Serially diluted C44Mab-34 was treated with CHO/CD44v3–10 and HSC-3 cells. The cells were further incubated with Alexa Fluor 488-conjugated anti-mouse IgG (1:200). Fluorescence data were collected using BD FACSLyric and analyzed using BD FACSuite software version 1.3 (BD Biosciences). The dissociation constant (K_D) was determined by GraphPad Prism 8 (the fitting binding isotherms to built-in one-site binding models; GraphPad Software, Inc., La Jolla, CA, USA).

2.8. Western blot analysis

The total cell lysates (10 μg of protein) were separated on 7.5% or 5%–20% polyacrylamide gels (FUJIFILM Wako Pure Chemical Corporation, Osaka, Japan) and transferred onto polyvinylidene difluoride (PVDF) membranes (Merck KGaA, Darmstadt, Germany). After blocking with 4% skim milk (Nacalai Tesque, Inc.) in PBST, the membranes were incubated with 10 μg/mL of C44Mab-34, 10 μg/mL of C44Mab-46, 1 μg/mL of NZ-1, or 1 μg/mL of an anti-β-actin mAb (clone AC-15; Sigma-Aldrich Corp.), and then incubated with peroxidase-conjugated anti-mouse immunoglobulins (diluted 1:1000; Agilent Technologies, Inc.) for C44Mab-34, C44Mab-46, and anti-β-actin. The chemiluminescence signals were obtained with ImmunoStar LD (FUJIFILM Wako Pure Chemical Corporation), and detected using a Sayaca-Imager (DRC Co. Ltd., Tokyo, Japan).

2.9. Immunohistochemical analysis

Formalin-fixed paraffin-embedded (FFPE) sections of the OSCC tissue array (Catalog number: OR601c) were purchased from US Biomax Inc. (Rockville, MD, USA). The OSCC tissue array was autoclaved in EnVision FLEX Target Retrieval Solution High pH (Agilent Technologies, Inc.) for 20 min. After blocking with SuperBlock T20 (Thermo Fisher Scientific, Inc.), the sections were incubated with C44Mab-34 (10 μg/mL) and C44Mab-46 (1 μg/mL) for 1 h at room temperature and then treated with the EnVision+ Kit for mouse (Agilent Technologies Inc.) for 30 min. The color was developed using 3,3′-diaminobenzidine tetrahydrochloride (DAB; Agilent Technologies Inc.). Hematoxylin (FUJIFILM Wako Pure Chemical Corporation) was used for the counterstaining. Leica DMD108 (Leica Microsystems GmbH, Wetzlar, Germany) was used to examine the sections and obtain images.

Preprints (www.preprints.org) | NOT PEER-REVIEWED | Posted: 27 February 2023 doi:10.20944/preprints202302.0437.v1

3. Results

3.1. Development of an anti-CD44v7/8 mAb, C44Mab-34

In this study, we purified human CD44ec as an immunogen (Figure. 1). One mouse was immunized with CD44ec, and hybridomas were seeded into 96-well plates. The supernatants were first screened by the reactivity to CD44ec by ELISA. Subsequently, the supernatants, which are positive for CHO/CD44v3–10 cells and negative for CHO-K1 cells, were further selected using the flow cytometry-based high throughput screening. By limiting dilution, anti-CD44 mAb-producing clones were finally established. Among them, C44Mab-34 (IgG1, kappa) was shown to recognize CD44p421–440 (GHQAGRRMDMDSSHSTTLQP), which are corresponding to variant 7 and 8-encoded sequence (supplementary Table S1). In contrast, C44Mab-34 never recognized other CD44v3-10 extracellular regions. These results indicated that C44Mab-34 specifically recognizes the border region between variant 7 and 8.

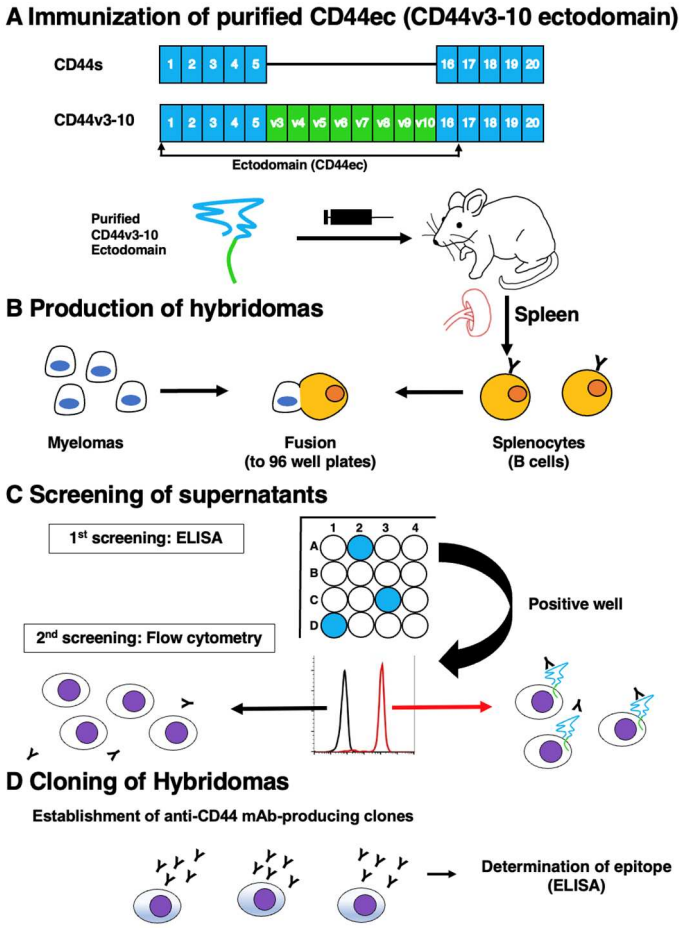

Figure 1. A schematic illustration of ant-human CD44 mAbs production. **(A)** Purified CD44v3–10 ectodomain was intraperitoneally injected into BALB/c mouse. **(B)** Hybridomas were produced by fusion of the splenocytes and P3U1 cells **(C)** The screening was performed by enzyme-linked immunosorbent assay (ELISA) and flow cytometry using parental CHO-K1 and CHO/CD44v3–10 cells. **(D)** After cloning and additional screening, a clone C44Mab-34 (IgG1, kappa) was established. Furthermore, the binding epitopes were determined by ELISA using peptides, which cover the extracellular domain of CD44v3–10.

3.2. Flow Cytometric Analysis of C44Mab-34 to CD44-Expressing Cells

We next investigated the reactivity of C44Mab-34 against CHO/CD44v3–10 and CHO/CD44s cells by flow cytometry. As shown in Figure 2A, C44Mab-34 recognized CHO/CD44v3–10 cells in a dose-

Preprints (www.preprints.org) | NOT PEER-REVIEWED | Posted: 27 February 2023 doi:10.20944/preprints202302.0437.v1

dependent manner, but neither CHO/CD44s (Figure 2B) nor CHO-K1 (Figure 2C) cells. The CHO/CD44s cells were recognized by an anti-pan-CD44 mAb C44Mab-46 [29] (Supplemental Figure S1). Furthermore, C44Mab-34 also recognized OSCC cell line, such as HSC-3 (Figure 2D) in a dose-dependent manner.

Next, we determined the binding affinity of C44Mab-34 with CHO/CD44v3–10 and HSC-3 using flow cytometry. The K_D of CHO/CD44v3–10 and HSC-3 was 1.4×10^{-9} M and 3.2×10^{-9} M, respectively, indicating that C44Mab-34 possesses moderate affinity for CD44v3–10-expressing cells (Figure 3).

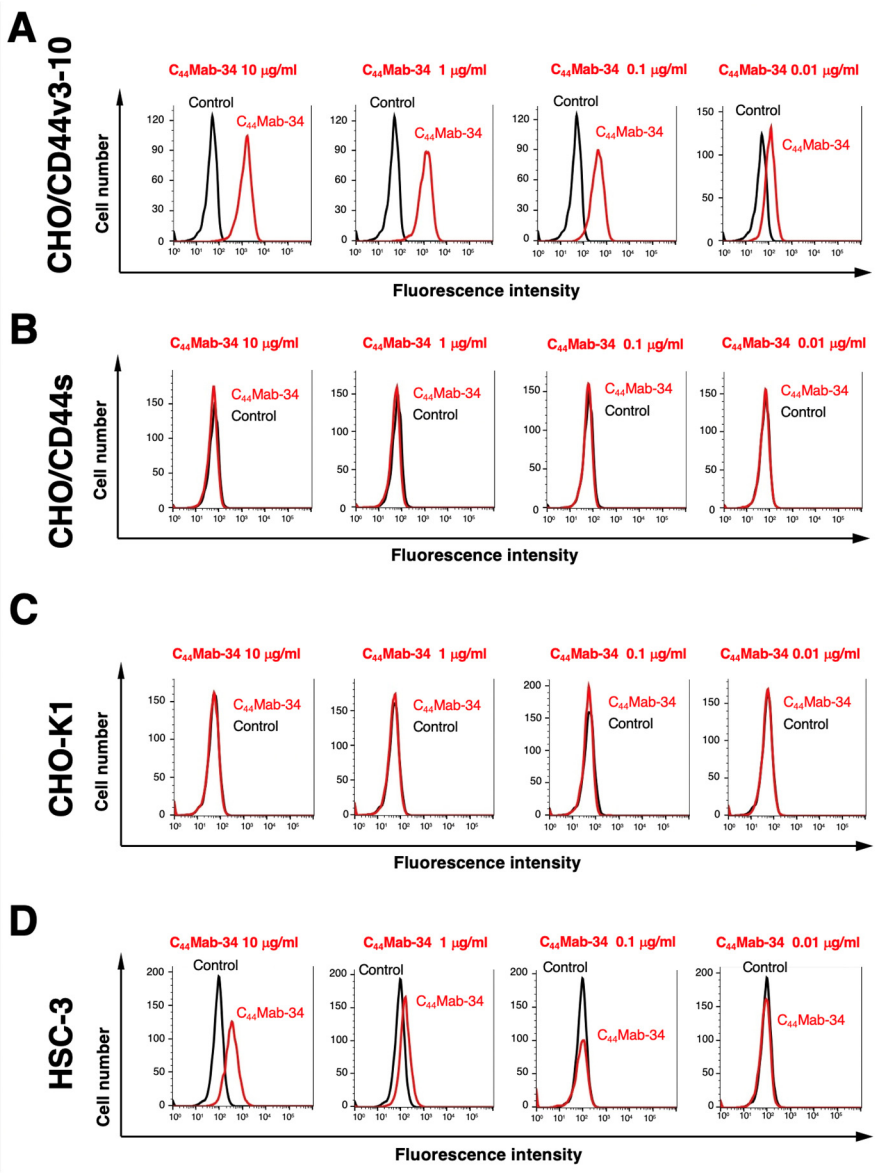

Figure 2. Flow cytometry using C44Mab-34 against CD44-expressing cells. CHO/CD44v3–10 (**A**), CHO/CD44s (**B**), CHO-K1 (**C**), and HSC-3 (**D**) cells were treated with 0.01-10 μg/mL of C44Mab-34, followed by treatment with Alexa Fluor 488-conjugated anti-mouse IgG (Red line). The black line represents the negative control (blocking buffer).

Preprints (www.preprints.org) | NOT PEER-REVIEWED | Posted: 27 February 2023 doi:10.20944/preprints202302.0437.v1

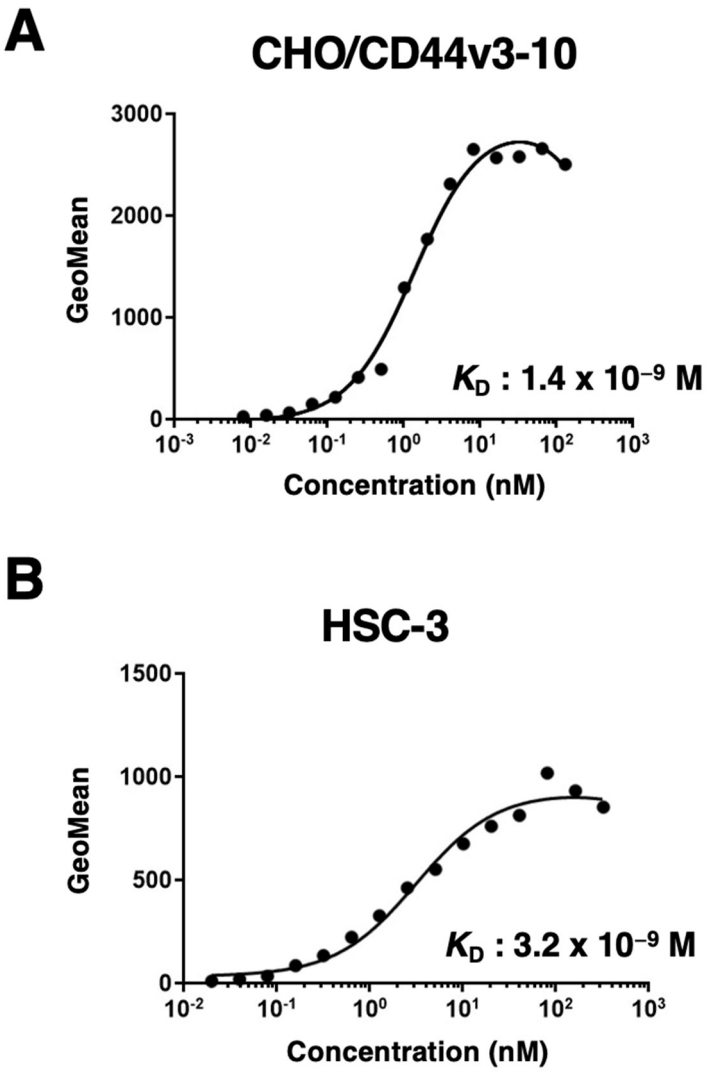

Figure 3. The binding affinity of C44Mab-34 to CD44-expressing cells. CHO/CD44v3–10 (**A**) and HSC-3 (**B**) cells were suspended in 100 μL of serially diluted C44Mab-34 at indicated concentrations. Then, cells were treated with Alexa Fluor 488-conjugated anti-mouse IgG. Fluorescence data were subsequently collected, followed by the calculation of the apparent dissociation constant (*K*D) by GraphPad PRISM 8.

3.3. Western Blot Analysis

We next performed western blot analysis to assess the sensitivity of C44Mab-34. Total cell lysates of CHO-K1, CHO/CD44s, and CHO/CD44v3–10 were analyzed. As shown in Figure 4A, an anti-pan-CD44 mAb, C44Mab-46, recognized the lysates from both CHO/CD44s (75~100 kDa) and CHO/CD44v3–10 (> 180 kDa). C44Mab-34 detected CD44v3–10 as more than 180-kDa bands. However, C44Mab-34 did not detect any bands from lysates of CHO-K1 and CHO/CD44s cells (Figure 4B). These results indicated that C44Mab-34 specifically detects CD44v3–10.

Preprints (www.preprints.org) | NOT PEER-REVIEWED | Posted: 27 February 2023 doi:10.20944/preprints202302.0437.v1

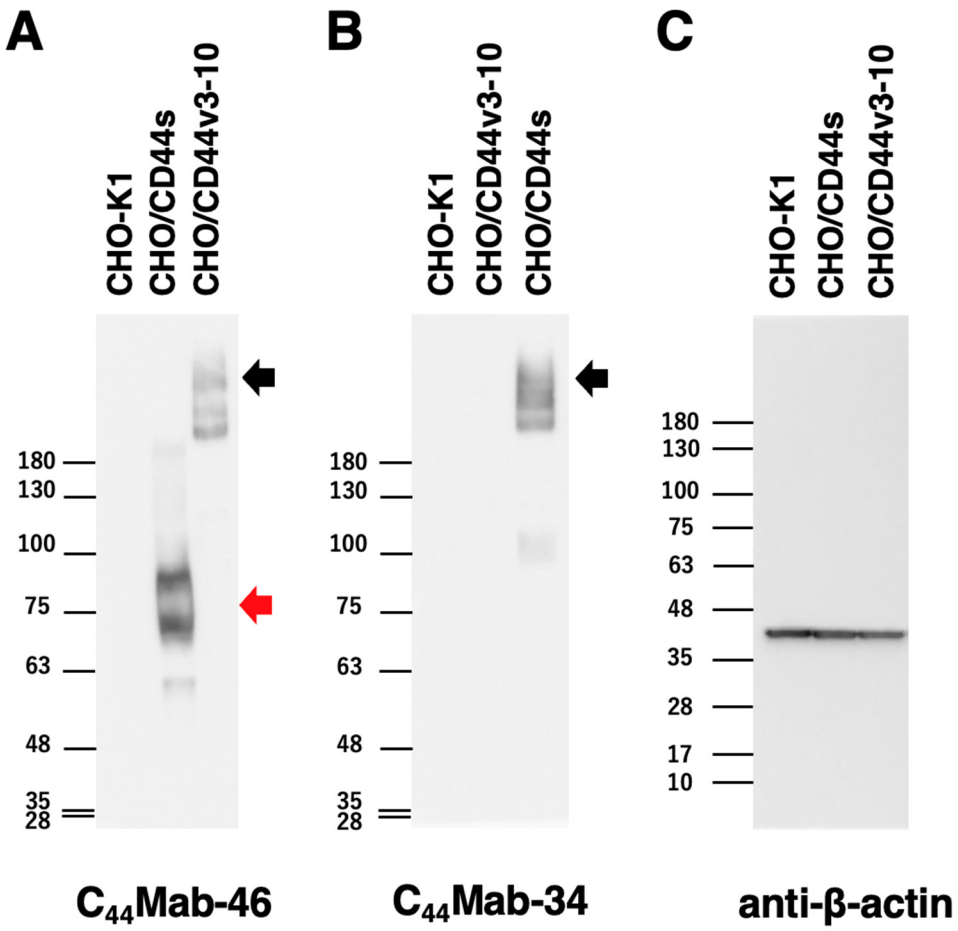

Figure 4. Western blot analysis using C44Mab-34. The cell lysates from CHO-K1, CHO/CD44s, and CHO/CD44v3–10 (10 μg) were electrophoresed and transferred onto polyvinylidene fluoride (PVDF) membranes. The membranes were incubated with 10 μg/mL of C44Mab-46 (**A**), 10 μg/mL of C44Mab-34 (**B**), and 1 μg/mL of an anti-β-actin mAb (**C**). Then, the membranes were incubated with anti-mouse immunoglobulins conjugated with peroxidase for C44Mab-46, C44Mab-34, and an anti-β-actin mAb. The red arrows indicate the CD44s (75~100 kDa). The black arrows indicate the CD44v3–10.

3.4. Immunohistochemical Analysis Using C44Mab-34 against Tumor Tissues

We next examined whether C44Mab-34 could be used for immunohistochemical analyses using FFPE sections. We used sequential sections of OSCC tissue microarray. In a well-differentiated OSCC section, the clear membranous staining in OSCC was observed by C44Mab-34 and C44Mab-46 (Figure. 5A, B). In an OSCC section with the stromal invaded phenotype, C44Mab-34 strongly stained stromal invaded OSCC and could clearly distinguish tumor cells from stromal tissues (Figure. 5C). In contrast, C44Mab-46 stained both invaded tumor cells and surrounding stroma cells (Figure. 5D). In Figure. 5E and F, C44Mab-34 and C44Mab-46 never stained tumor tissue, but clear stromal staining was observed by C44Mab-46 (Figure. 5F). We summarized the data of immunohistochemical analysis in Table 1; C44Mab-34 stained 42 out of 49 (86%) cases of OSCC. These results indicated that C44Mab-34 is useful for immunohistochemical analysis of FFPE tumor sections.

Preprints (www.preprints.org) | NOT PEER-REVIEWED | Posted: 27 February 2023 doi:10.20944/preprints202302.0437.v1

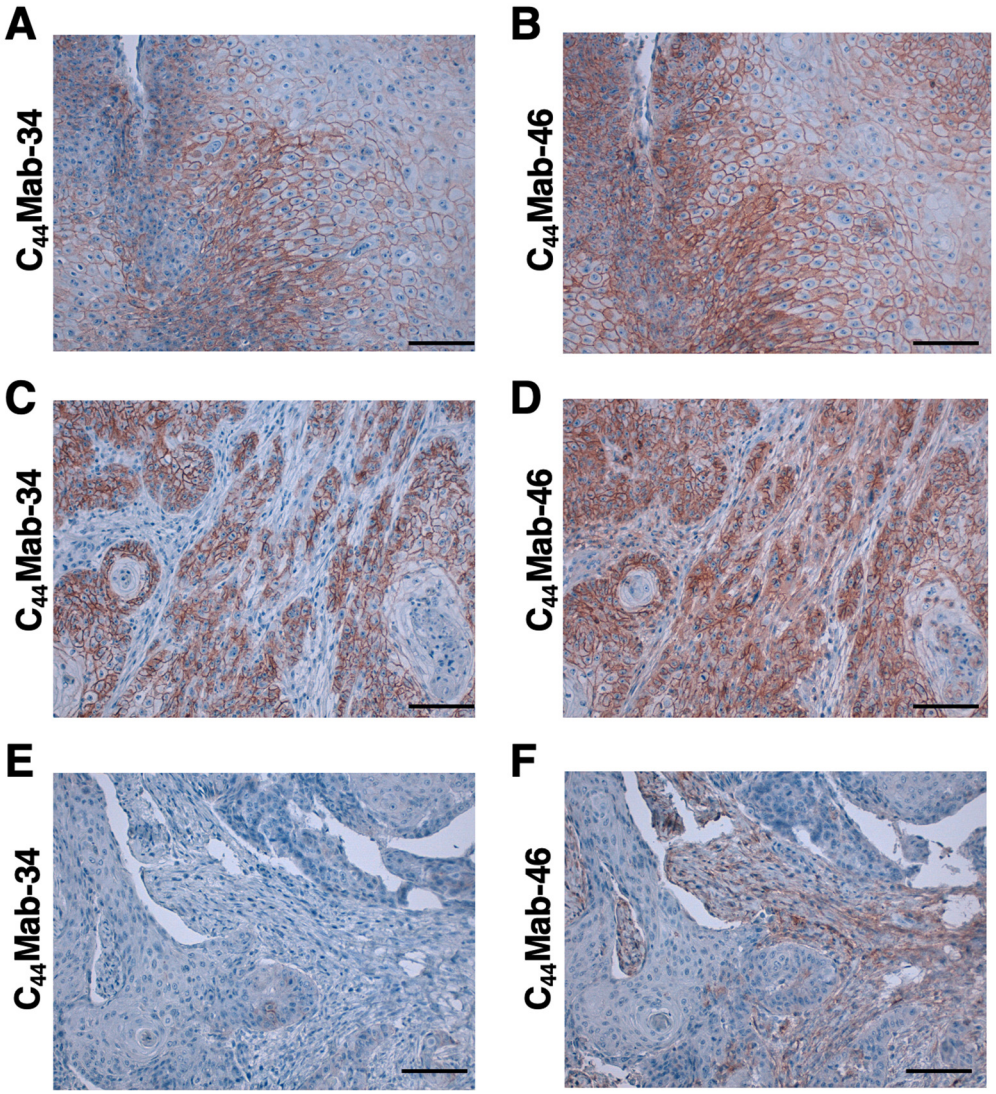

Figure 5. Immunohistochemical analysis using C44Mab-34 and C44Mab-46 against OSCC tissues. After antigen retrieval, serial sections of OSCC tissue array (Catalog number: OR601c) were incubated with 10 μg/mL of C44Mab-34 or 1 μg/mL of C44Mab-46 followed by treatment with the Envision+ kit. The color was developed using 3,3′-diaminobenzidine tetrahydrochloride (DAB), and the sections were counterstained with hematoxylin. Scale bar = 100 μm.

Table 1. Immunohistochemical analysis using C44Mab-34 and C44Mab-46 against an OSCC tissue array.

No	Age	Sex	Organ/Anatomic Site	Pathology diagnosis	TNM	C44Mab-34	C44Mab-46
1	78	M	Tongue	Squamous cell carcinoma of tongue	T2N0M0	+	+
2	40	M	Tongue	Squamous cell carcinoma of tongue	T2N0M0	+	++
3	35	F	Tongue	Squamous cell carcinoma of tongue	T2N0M0	+++	++
4	61	M	Tongue	Squamous cell carcinoma of tongue	T2N0M0	+++	+++
5	41	F	Tongue	Squamous cell carcinoma of tongue	T2N0M0	+	+

Preprints (www.preprints.org) | NOT PEER-REVIEWED | Posted: 27 February 2023 doi:10.20944/preprints202302.0437.v1

6	64	M	Tongue	Squamous cell carcinoma of right tongue	T2N2M0	+	++
7	76	M	Tongue	Squamous cell carcinoma of tongue	T1N0M0	+	++
8	50	F	Tongue	Squamous cell carcinoma of tongue	T2N0M0	+++	++
9	44	M	Tongue	Squamous cell carcinoma of tongue	T2N1M0	+++	++
10	53	F	Tongue	Squamous cell carcinoma of tongue	T1N0M0	+	++
11	46	F	Tongue	Squamous cell carcinoma of tongue	T2N0M0	-	+
12	50	M	Tongue	Squamous cell carcinoma of root of tongue	T3N1M0	+++	+
13	36	F	Tongue	Squamous cell carcinoma of tongue	T1N0M0	+++	+++
14	63	F	Tongue	Squamous cell carcinoma of tongue	T1N0M0	+	+
15	46	M	Tongue	Squamous cell carcinoma of tongue	T2N0M0	++	-
16	58	M	Tongue	Squamous cell carcinoma of tongue	T2N0M0	+	+
17	64	M	Lip	Squamous cell carcinoma of lower lip	T1N0M0	+++	+++
18	57	M	Lip	Squamous cell carcinoma of lower lip	T2N0M0	++	+++
19	61	M	Lip	Squamous cell carcinoma of lower lip	T1N0M0	+++	++
20	60	M	Gum	Squamous cell carcinoma of gum	T3N0M0	+	+
21	60	M	Gum	Squamous cell carcinoma of gum	T1N0M0	+++	+++
22	69	M	Gum	Squamous cell carcinoma of upper gum	T3N0M0	+	++
23	53	M	Bucca cavioris	Squamous cell carcinoma of bucca cavioris	T2N0M0	++	+
24	55	M	Bucca cavioris	Squamous cell carcinoma of bucca cavioris	T1N0M0	++	+
25	58	M	Tongue	Squamous cell carcinoma of base of tongue	T1N0M0	+	++
26	63	M	Oral cavity	Squamous cell carcinoma	T1N0M0	++	++
27	48	F	Tongue	Squamous cell carcinoma of tongue	T1N0M0	++	+
28	80	M	Lip	Squamous cell carcinoma of lower lip	T1N0M0	+++	+++
29	77	M	Tongue	Squamous cell carcinoma of base of tongue	T2N0M0	+++	++
30	59	M	Tongue	Squamous cell carcinoma of tongue	T2N0M0	++	-

Preprints (www.preprints.org) | NOT PEER-REVIEWED | Posted: 27 February 2023 doi:10.20944/preprints202302.0437.v1

31	77	F	Tongue	Squamous cell carcinoma of tongue	T1N0M0	+	++
32	56	M	Tongue	Squamous cell carcinoma of root of tongue	T2N1M0	+	+
33	60	M	Tongue	Squamous cell carcinoma of tongue	T2N1M0	+	++
34	62	M	Tongue	Squamous cell carcinoma of tongue	T2N0M0	+++	++
35	67	F	Tongue	Squamous cell carcinoma of tongue	T2N0M0	+++	++
36	47	F	Tongue	Squamous cell carcinoma of tongue	T2N0M0	+++	+++
37	37	M	Tongue	Squamous cell carcinoma of tongue	T2N1M0	-	-
38	55	F	Tongue	Squamous cell carcinoma of tongue	T2N0M0	++	++
39	56	F	Bucca cavioris	Squamous cell carcinoma of bucca cavioris	T2N0M0	++	+
40	49	M	Bucca cavioris	Squamous cell carcinoma of bucca cavioris	T1N0M0	-	-
41	45	M	Bucca cavioris	Squamous cell carcinoma of bucca cavioris	T2N0M0	-	-
42	42	M	Bucca cavioris	Squamous cell carcinoma of bucca cavioris	T3N0M0	++	++
43	44	M	Jaw	Squamous cell carcinoma of right drop jaw	T1N0M0	+	+++
44	40	F	Tongue	Squamous cell carcinoma of base of tongue	T2N0M0	-	++
45	49	M	Bucca cavioris	Squamous cell carcinoma of bucca cavioris	T1N0M0	+++	+++
46	56	F	Tongue	Squamous cell carcinoma of base of tongue	T2N0M0	-	-
47	42	M	Bucca cavioris	Squamous cell carcinoma of bucca cavioris	T3N0M0	+++	+++
48	87	F	Face	Squamous cell carcinoma of left face	T2N0M0	+	+
49	50	M	Gum	Squamous cell carcinoma of gum	T2N0M0	-	-

4. Discussion

Head and neck cancer is the seventh most common type of cancer worldwide, and exhibits aggressive development in clinic [58]. Head and neck cancer remains a complex disease with a profound impact on patients and their quality of life after surgical ablation and therapies. The knowledge of disease has been accumulated with regard to tumor biology and the prevention, and therapeutic options have been simultaneously developed [58]. HNSCC is the most common type of head and neck cancer, and revealed as the second highest CD44-expressing cancer type in the Pan-Cancer Atlas [59]. The CD44 overexpression is associated with poor prognosis and resistance to therapy [60-62]. The reduced CD44 expression leads to the growth suppression of tumor cells [17,63]. Therefore, CD44 has been considered as an important target for mAb therapies. In this study, we developed a novel anti-CD44v7/8 mAb, C$_{44}$Mab-34, and showed the multiple applications to flow

 doi:10.20944/preprints202302.0437.v1

cytometry (Figure 2 and 3), western blotting (Figure 4), and immunohistochemistry of OSCC (Figure 5).

An anti-CD44v7/8 mAb (clone VFF-17) was previously developed and mainly used for the immunohistochemistry of normal tissue and tumors [64,65]. The epitope of VFF-17 mAb was determined by binding studies with fusion proteins encoding v7 or v8 exons either alone or in combination [66]. However, detailed amino acid sequence of the epitope has not been determined. As shown in supplementary Table S1, C$_{44}$Mab-34 recognized CD44p421–440 [GHQAGRRMD (included in v7) + MDSSHSTTLQP (included in v8)]. In contrast, C$_{44}$Mab-34 never recognized both CD44p411–430 [FNPISHPMGRGHQAGRRMD (included in v7) + M (included in v8)] and CD44p431–450 [DSSHSTTLQPTANPNTGLVE (included in v8)]. These results suggest that C$_{44}$Mab-34 recognized the border sequence between v7 and v8. In addition, CD44 is known to be heavily glycosylated [67], and the glycosylation pattern is thought to depend on the host cells. Since the epitope of C$_{44}$Mab-34 contains predicted and confirmed *O*-glycan sites [67], further studies are needed whether the recognition of C$_{44}$Mab-34 is affected by the glycosylation.

ΔNp63 is known as a marker of basal cells of stratified epithelium and SCC [68]. ΔNp63 mediates HA metabolism and signaling [69]. Especially, ΔNp63 directly bind to the p63-binding sequence on the promoter region and the first intron of CD44 gene, respectively [69]. Therefore, ΔNp63 is thought to be one of the important regulators of CD44 in SCC. In whole-exome sequencing data analysis from 74 HNSCC-normal pairs, ΔNp63-encoded gene, *TP63*, was identified as a significantly mutated genes, which results in the activation of ΔNp63 pathway [70]. The relationship between ΔNp63 activation and CD44 transcription should be investigated in the future study. Furthermore, the mechanism of the variant 7/8 inclusion by alternative splicing remains to be determined.

In clinical studies, an anti-pan CD44 mAb, RG7356 demonstrated some efficacy and an acceptable safety profile in phase 1 studies. However, the study was terminated due to no evidence of a clinical and pharmacodynamic dose-response relationship with RG7356 [71]. Furthermore, a variant 6-specific CD44 mAb-drug conjugate (bivatuzumab−mertansine) was also evaluated in clinical trials. However, lethal toxic epidermal necrolysis halted further development. The efficient accumulation of mertansine in skin was most likely responsible for the high toxicity [72,73]. Therefore, therapeutic effects of CD44 mAbs have been disappointing until now.

Near-infrared photoimmunotherapy (NIR-PIT) is a novel tumor therapy that uses a targeted mAb–photoabsorber conjugate (APC) [74]. The mAb binds to the targeted cell surface antigen, and the photoactivatable dye, IRDye700DX (IR700), induces disruption of cellular membrane after NIR-light exposure. Since NIR-light exposure can be performed at tumor sites locally, APC can exert antitumor effect selectivity, while minimizing damage to surrounding tissue [75,76]. Preclinical studies indicate that NIR-PIT induces tumor necrosis and immunogenic cell death that can lead to local and systemic induction of innate and adaptive immunity [77]. A first-in-human phase I and II trial of NIR-PIT with RM-1929 (an anti-epidermal growth factor receptor mAb, cetuximab-IR700 conjugate) in patients with inoperable HNSCC was conducted and exhibited the efficacy [78].

A preclinical study of the anti-CD44 mAb-based NIR-PIT was reported [79]. The study used anti-mouse/human pan-CD44 mAb, IM7, conjugated with IR700 (CD44–IR700) in syngeneic mouse model of OSCC. The CD44–IR700 can induce significant antitumor responses after a single injection of the conjugate and NIR light exposure in CD44 expressing OSCC tumors [79]. As shown in Figure 5D and F, a pan-CD44 mAb, C$_{44}$Mab-46 recognized not only tumor cells, but also stromal tissue, and probably immune cells which are important for antitumor immunity. Therefore, CD44v is a promising tumor antigen for NIR-PIT, which could be a new modality for OSCC with locoregional recurrence.

We previously produced recombinant antibodies which are converted to mouse IgG$_{2a}$ subclass from mouse IgG$_1$. Furthermore, we produced a defucosylated IgG$_{2a}$ mAbs using fucosyltransferase 8-deficient CHO-K1 cells to potentiate the antibody-dependent cellular cytotoxicity. The defucosylated mAbs showed potent antitumor activity in mouse xenograft models [33,80-86]. Therefore, a class-switched and defucosylated version of C$_{44}$Mab-34 is required to evaluate the antitumor activity *in vivo*.

Supplementary Materials: Table S1, The determination of the binding epitope of C44Mab-34 by ELISA. Figure S1, Recognition of CHO/CD44s and CHO/CD44v3–10 by C44Mab-46 by flow cytometry.

Author Contributions: K.O, H.S., and T.T. performed the experiments. M.K.K. and Y.K. designed the experiments. H.S. and K.O analyzed the data. K.O., H.S. and Y.K. wrote the manuscript. All authors have read and agreed to the manuscript.

Funding: This research was supported in part by Japan Agency for Medical Research and Development (AMED) under Grant Numbers: JP22ama121008 (to Y.K.), JP22am0401013 (to Y.K.), JP22bm1004001 (to Y.K.), JP22ck0106730 (to Y.K.), and JP21am0101078 (to Y.K.), and by the Japan Society for the Promotion of Science (JSPS) Grants-in-Aid for Scientific Research (KAKENHI) grant nos. 21K20789 (to T.T.), 22K06995 (to H.S.), 21K07168 (to M.K.K.), and 22K07224 (to Y.K.).

Institutional Review Board Statement: The animal study protocol was approved by the Animal Care and Use Committee of Tohoku University (Permit number: 2019NiA-001) for studies involving animals.

Data Availability Statement: The data presented in this study are available in the article and supplementary material.

Conflicts of Interest: The authors have no conflicts of interest to declare.

References

1. Johnson, D.E.; Burtness, B.; Leemans, C.R.; Lui, V.W.Y.; Bauman, J.E.; Grandis, J.R. Head and neck squamous cell carcinoma. *Nat Rev Dis Primers* **2020**, *6*, 92, doi:10.1038/s41572-020-00224-3.
2. Siegel, R.L.; Miller, K.D.; Wagle, N.S.; Jemal, A. Cancer statistics, 2023. *CA Cancer J Clin* **2023**, *73*, 17-48, doi:10.3322/caac.21763.
3. Kang, J.J.; Yu, Y.; Chen, L.; Zakeri, K.; Gelblum, D.Y.; McBride, S.M.; Riaz, N.; Tsai, C.J.; Kriplani, A.; Hung, T.K.W.; et al. Consensuses, controversies, and future directions in treatment deintensification for human papillomavirus-associated oropharyngeal cancer. *CA Cancer J Clin* **2022**, doi:10.3322/caac.21758.
4. Jemal, A.; Siegel, R.; Ward, E.; Hao, Y.; Xu, J.; Murray, T.; Thun, M.J. Cancer statistics, 2008. *CA Cancer J Clin* **2008**, *58*, 71-96, doi:10.3322/ca.2007.0010.
5. Xing, D.T.; Khor, R.; Gan, H.; Wada, M.; Ermongkonchai, T.; Ng, S.P. Recent Research on Combination of Radiotherapy with Targeted Therapy or Immunotherapy in Head and Neck Squamous Cell Carcinoma: A Review for Radiation Oncologists. *Cancers (Basel)* **2021**, *13*, doi:10.3390/cancers13225716.
6. Muzaffar, J.; Bari, S.; Kirtane, K.; Chung, C.H. Recent Advances and Future Directions in Clinical Management of Head and Neck Squamous Cell Carcinoma. *Cancers (Basel)* **2021**, *13*, doi:10.3390/cancers13020338.
7. Maitland, N.J.; Collins, A.T. Cancer stem cells - A therapeutic target? *Curr Opin Mol Ther* **2010**, *12*, 662-673.
8. Prince, M.E.; Ailles, L.E. Cancer stem cells in head and neck squamous cell cancer. *J Clin Oncol* **2008**, *26*, 2871-2875, doi:10.1200/jco.2007.15.1613.
9. Ailles, L.E.; Weissman, I.L. Cancer stem cells in solid tumors. *Curr Opin Biotechnol* **2007**, *18*, 460-466, doi:10.1016/j.copbio.2007.10.007.
10. Keysar, S.B.; Le, P.N.; Miller, B.; Jackson, B.C.; Eagles, J.R.; Nieto, C.; Kim, J.; Tang, B.; Glogowska, M.J.; Morton, J.J.; et al. Regulation of Head and Neck Squamous Cancer Stem Cells by PI3K and SOX2. *J Natl Cancer Inst* **2017**, *109*, doi:10.1093/jnci/djw189.
11. de Miranda, M.C.; Melo, M.I.A.; Cunha, P.D.S.; Gentilini, J.J.; Faria, J.; Rodrigues, M.A.; Gomes, D.A. Roles of mesenchymal stromal cells in the head and neck cancer microenvironment. *Biomed Pharmacother* **2021**, *144*, 112269, doi:10.1016/j.biopha.2021.112269.
12. Yu, S.S.; Cirillo, N. The molecular markers of cancer stem cells in head and neck tumors. *J Cell Physiol* **2020**, *235*, 65-73, doi:10.1002/jcp.28963.
13. Tahmasebi, E.; Alikhani, M.; Yazdanian, A.; Yazdanian, M.; Tebyanian, H.; Seifalian, A. The current markers of cancer stem cell in oral cancers. *Life Sci* **2020**, *249*, 117483, doi:10.1016/j.lfs.2020.117483.
14. Prince, M.E.; Sivanandan, R.; Kaczorowski, A.; Wolf, G.T.; Kaplan, M.J.; Dalerba, P.; Weissman, I.L.; Clarke, M.F.; Ailles, L.E. Identification of a subpopulation of cells with cancer stem cell properties in head and neck squamous cell carcinoma. *Proc Natl Acad Sci U S A* **2007**, *104*, 973-978, doi:10.1073/pnas.0610117104.
15. Lee, Y.; Shin, J.H.; Longmire, M.; Wang, H.; Kohrt, H.E.; Chang, H.Y.; Sunwoo, J.B. CD44+ Cells in Head and Neck Squamous Cell Carcinoma Suppress T-Cell-Mediated Immunity by Selective Constitutive and Inducible Expression of PD-L1. *Clin Cancer Res* **2016**, *22*, 3571-3581, doi:10.1158/1078-0432.Ccr-15-2665.
16. Davis, S.J.; Divi, V.; Owen, J.H.; Bradford, C.R.; Carey, T.E.; Papagerakis, S.; Prince, M.E. Metastatic potential of cancer stem cells in head and neck squamous cell carcinoma. *Arch Otolaryngol Head Neck Surg* **2010**, *136*, 1260-1266, doi:10.1001/archoto.2010.219.
17. Ponta, H.; Sherman, L.; Herrlich, P.A. CD44: from adhesion molecules to signalling regulators. *Nat Rev Mol Cell Biol* **2003**, *4*, 33-45, doi:10.1038/nrm1004.

18. Yan, Y.; Zuo, X.; Wei, D. Concise Review: Emerging Role of CD44 in Cancer Stem Cells: A Promising Biomarker and Therapeutic Target. *Stem Cells Transl Med* **2015**, *4*, 1033-1043, doi:10.5966/sctm.2015-0048.
19. Slevin, M.; Krupinski, J.; Gaffney, J.; Matou, S.; West, D.; Delisser, H.; Savani, R.C.; Kumar, S. Hyaluronan-mediated angiogenesis in vascular disease: uncovering RHAMM and CD44 receptor signaling pathways. *Matrix Biol* **2007**, *26*, 58-68, doi:10.1016/j.matbio.2006.08.261.
20. Naor, D.; Wallach-Dayan, S.B.; Zahalka, M.A.; Sionov, R.V. Involvement of CD44, a molecule with a thousand faces, in cancer dissemination. *Semin Cancer Biol* **2008**, *18*, 260-267, doi:10.1016/j.semcancer.2008.03.015.
21. Günthert, U.; Hofmann, M.; Rudy, W.; Reber, S.; Zöller, M.; Haussmann, I.; Matzku, S.; Wenzel, A.; Ponta, H.; Herrlich, P. A new variant of glycoprotein CD44 confers metastatic potential to rat carcinoma cells. *Cell* **1991**, *65*, 13-24, doi:10.1016/0092-8674(91)90403-l.
22. Guo, Q.; Yang, C.; Gao, F. The state of CD44 activation in cancer progression and therapeutic targeting. *Febs j* **2021**, doi:10.1111/febs.16179.
23. Hassn Mesrati, M.; Syafruddin, S.E.; Mohtar, M.A.; Syahir, A. CD44: A Multifunctional Mediator of Cancer Progression. *Biomolecules* **2021**, *11*, doi:10.3390/biom11121850.
24. Morath, I.; Hartmann, T.N.; Orian-Rousseau, V. CD44: More than a mere stem cell marker. *Int J Biochem Cell Biol* **2016**, *81*, 166-173, doi:10.1016/j.biocel.2016.09.009.
25. Bennett, K.L.; Jackson, D.G.; Simon, J.C.; Tanczos, E.; Peach, R.; Modrell, B.; Stamenkovic, I.; Plowman, G.; Aruffo, A. CD44 isoforms containing exon V3 are responsible for the presentation of heparin-binding growth factor. *J Cell Biol* **1995**, *128*, 687-698, doi:10.1083/jcb.128.4.687.
26. Orian-Rousseau, V.; Chen, L.; Sleeman, J.P.; Herrlich, P.; Ponta, H. CD44 is required for two consecutive steps in HGF/c-Met signaling. *Genes Dev* **2002**, *16*, 3074-3086, doi:10.1101/gad.242602.
27. Ishimoto, T.; Nagano, O.; Yae, T.; Tamada, M.; Motohara, T.; Oshima, H.; Oshima, M.; Ikeda, T.; Asaba, R.; Yagi, H.; et al. CD44 variant regulates redox status in cancer cells by stabilizing the xCT subunit of system xc(-) and thereby promotes tumor growth. *Cancer Cell* **2011**, *19*, 387-400, doi:10.1016/j.ccr.2011.01.038.
28. Yamada, S.; Itai, S.; Nakamura, T.; Yanaka, M.; Kaneko, M.K.; Kato, Y. Detection of high CD44 expression in oral cancers using the novel monoclonal antibody, C(44)Mab-5. *Biochem Biophys Rep* **2018**, *14*, 64-68, doi:10.1016/j.bbrep.2018.03.007.
29. Goto, N.; Suzuki, H.; Tanaka, T.; Asano, T.; Kaneko, M.K.; Kato, Y. Development of a Novel Anti-CD44 Monoclonal Antibody for Multiple Applications against Esophageal Squamous Cell Carcinomas. *Int J Mol Sci* **2022**, *23*, doi:10.3390/ijms23105535.
30. Takei, J.; Asano, T.; Suzuki, H.; Kaneko, M.K.; Kato, Y. Epitope Mapping of the Anti-CD44 Monoclonal Antibody (C44Mab-46) Using Alanine-Scanning Mutagenesis and Surface Plasmon Resonance. *Monoclon Antib Immunodiagn Immunother* **2021**, *40*, 219-226, doi:10.1089/mab.2021.0028.
31. Asano, T.; Kaneko, M.K.; Takei, J.; Tateyama, N.; Kato, Y. Epitope Mapping of the Anti-CD44 Monoclonal Antibody (C44Mab-46) Using the REMAP Method. *Monoclon Antib Immunodiagn Immunother* **2021**, *40*, 156-161, doi:10.1089/mab.2021.0012.
32. Asano, T.; Kaneko, M.K.; Kato, Y. Development of a Novel Epitope Mapping System: RIEDL Insertion for Epitope Mapping Method. *Monoclon Antib Immunodiagn Immunother* **2021**, *40*, 162-167, doi:10.1089/mab.2021.0023.
33. Takei, J.; Kaneko, M.K.; Ohishi, T.; Hosono, H.; Nakamura, T.; Yanaka, M.; Sano, M.; Asano, T.; Sayama, Y.; Kawada, M.; et al. A defucosylated antiCD44 monoclonal antibody 5mG2af exerts antitumor effects in mouse xenograft models of oral squamous cell carcinoma. *Oncol Rep* **2020**, *44*, 1949-1960, doi:10.3892/or.2020.7735.
34. Kato, Y.; Yamada, S.; Furusawa, Y.; Itai, S.; Nakamura, T.; Yanaka, M.; Sano, M.; Harada, H.; Fukui, M.; Kaneko, M.K. PMab-213: A Monoclonal Antibody for Immunohistochemical Analysis Against Pig Podoplanin. *Monoclon Antib Immunodiagn Immunother* **2019**, *38*, 18-24, doi:10.1089/mab.2018.0048.
35. Furusawa, Y.; Yamada, S.; Itai, S.; Sano, M.; Nakamura, T.; Yanaka, M.; Fukui, M.; Harada, H.; Mizuno, T.; Sakai, Y.; et al. PMab-210: A Monoclonal Antibody Against Pig Podoplanin. *Monoclon Antib Immunodiagn Immunother* **2019**, *38*, 30-36, doi:10.1089/mab.2018.0038.
36. Furusawa, Y.; Yamada, S.; Itai, S.; Nakamura, T.; Yanaka, M.; Sano, M.; Harada, H.; Fukui, M.; Kaneko, M.K.; Kato, Y. PMab-219: A monoclonal antibody for the immunohistochemical analysis of horse podoplanin. *Biochem Biophys Rep* **2019**, *18*, 100616, doi:10.1016/j.bbrep.2019.01.009.
37. Furusawa, Y.; Yamada, S.; Itai, S.; Nakamura, T.; Takei, J.; Sano, M.; Harada, H.; Fukui, M.; Kaneko, M.K.; Kato, Y. Establishment of a monoclonal antibody PMab-233 for immunohistochemical analysis against Tasmanian devil podoplanin. *Biochem Biophys Rep* **2019**, *18*, 100631, doi:10.1016/j.bbrep.2019.100631.
38. Kato, Y.; Kaneko, M.K.; Kuno, A.; Uchiyama, N.; Amano, K.; Chiba, Y.; Hasegawa, Y.; Hirabayashi, J.; Narimatsu, H.; Mishima, K.; et al. Inhibition of tumor cell-induced platelet aggregation using a novel anti-podoplanin antibody reacting with its platelet-aggregation-stimulating domain. *Biochem Biophys Res Commun* **2006**, *349*, 1301-1307, doi:10.1016/j.bbrc.2006.08.171.

39. Chalise, L.; Kato, A.; Ohno, M.; Maeda, S.; Yamamichi, A.; Kuramitsu, S.; Shiina, S.; Takahashi, H.; Ozone, S.; Yamaguchi, J.; et al. Efficacy of cancer-specific anti-podoplanin CAR-T cells and oncolytic herpes virus G47Delta combination therapy against glioblastoma. *Mol Ther Oncolytics* **2022**, *26*, 265-274, doi:10.1016/j.omto.2022.07.006.
40. Ishikawa, A.; Waseda, M.; Ishii, T.; Kaneko, M.K.; Kato, Y.; Kaneko, S. Improved anti-solid tumor response by humanized anti-podoplanin chimeric antigen receptor transduced human cytotoxic T cells in an animal model. *Genes Cells* **2022**, *27*, 549-558, doi:10.1111/gtc.12972.
41. Tamura-Sakaguchi, R.; Aruga, R.; Hirose, M.; Ekimoto, T.; Miyake, T.; Hizukuri, Y.; Oi, R.; Kaneko, M.K.; Kato, Y.; Akiyama, Y.; et al. Moving toward generalizable NZ-1 labeling for 3D structure determination with optimized epitope-tag insertion. *Acta Crystallogr D Struct Biol* **2021**, *77*, 645-662, doi:10.1107/S2059798321002527.
42. Kaneko, M.K.; Ohishi, T.; Nakamura, T.; Inoue, H.; Takei, J.; Sano, M.; Asano, T.; Sayama, Y.; Hosono, H.; Suzuki, H.; et al. Development of Core-Fucose-Deficient Humanized and Chimeric Anti-Human Podoplanin Antibodies. *Monoclon Antib Immunodiagn Immunother* **2020**, *39*, 167-174, doi:10.1089/mab.2020.0019.
43. Fujii, Y.; Matsunaga, Y.; Arimori, T.; Kitago, Y.; Ogasawara, S.; Kaneko, M.K.; Kato, Y.; Takagi, J. Tailored placement of a turn-forming PA tag into the structured domain of a protein to probe its conformational state. *J Cell Sci* **2016**, *129*, 1512-1522, doi:10.1242/jcs.176685.
44. Abe, S.; Kaneko, M.K.; Tsuchihashi, Y.; Izumi, T.; Ogasawara, S.; Okada, N.; Sato, C.; Tobiume, M.; Otsuka, K.; Miyamoto, L.; et al. Antitumor effect of novel anti-podoplanin antibody NZ-12 against malignant pleural mesothelioma in an orthotopic xenograft model. *Cancer Sci* **2016**, *107*, 1198-1205, doi:10.1111/cas.12985.
45. Kaneko, M.K.; Abe, S.; Ogasawara, S.; Fujii, Y.; Yamada, S.; Murata, T.; Uchida, H.; Tahara, H.; Nishioka, Y.; Kato, Y. Chimeric Anti-Human Podoplanin Antibody NZ-12 of Lambda Light Chain Exerts Higher Antibody-Dependent Cellular Cytotoxicity and Complement-Dependent Cytotoxicity Compared with NZ-8 of Kappa Light Chain. *Monoclon Antib Immunodiagn Immunother* **2017**, *36*, 25-29, doi:10.1089/mab.2016.0047.
46. Ito, A.; Ohta, M.; Kato, Y.; Inada, S.; Kato, T.; Nakata, S.; Yatabe, Y.; Goto, M.; Kaneda, N.; Kurita, K.; et al. A Real-Time Near-Infrared Fluorescence Imaging Method for the Detection of Oral Cancers in Mice Using an Indocyanine Green-Labeled Podoplanin Antibody. *Technol Cancer Res Treat* **2018**, *17*, 1533033818767936, doi:10.1177/1533033818767936.
47. Tamura, R.; Oi, R.; Akashi, S.; Kaneko, M.K.; Kato, Y.; Nogi, T. Application of the NZ-1 Fab as a crystallization chaperone for PA tag-inserted target proteins. *Protein Sci* **2019**, *28*, 823-836, doi:10.1002/pro.3580.
48. Shiina, S.; Ohno, M.; Ohka, F.; Kuramitsu, S.; Yamamichi, A.; Kato, A.; Motomura, K.; Tanahashi, K.; Yamamoto, T.; Watanabe, R.; et al. CAR T Cells Targeting Podoplanin Reduce Orthotopic Glioblastomas in Mouse Brains. *Cancer Immunol Res* **2016**, *4*, 259-268, doi:10.1158/2326-6066.CIR-15-0060.
49. Kuwata, T.; Yoneda, K.; Mori, M.; Kanayama, M.; Kuroda, K.; Kaneko, M.K.; Kato, Y.; Tanaka, F. Detection of Circulating Tumor Cells (CTCs) in Malignant Pleural Mesothelioma (MPM) with the "Universal" CTC-Chip and An Anti-Podoplanin Antibody NZ-1.2. *Cells* **2020**, *9*, doi:10.3390/cells9040888.
50. Nishinaga, Y.; Sato, K.; Yasui, H.; Taki, S.; Takahashi, K.; Shimizu, M.; Endo, R.; Koike, C.; Kuramoto, N.; Nakamura, S.; et al. Targeted Phototherapy for Malignant Pleural Mesothelioma: Near-Infrared Photoimmunotherapy Targeting Podoplanin. *Cells* **2020**, *9*, doi:10.3390/cells9041019.
51. Fujii, Y.; Kaneko, M.; Neyazaki, M.; Nogi, T.; Kato, Y.; Takagi, J. PA tag: a versatile protein tagging system using a super high affinity antibody against a dodecapeptide derived from human podoplanin. *Protein Expr Purif* **2014**, *95*, 240-247, doi:10.1016/j.pep.2014.01.009.
52. Kato, Y.; Kaneko, M.K.; Kunita, A.; Ito, H.; Kameyama, A.; Ogasawara, S.; Matsuura, N.; Hasegawa, Y.; Suzuki-Inoue, K.; Inoue, O.; et al. Molecular analysis of the pathophysiological binding of the platelet aggregation-inducing factor podoplanin to the C-type lectin-like receptor CLEC-2. *Cancer Sci* **2008**, *99*, 54-61, doi:10.1111/j.1349-7006.2007.00634.x.
53. Kato, Y.; Vaidyanathan, G.; Kaneko, M.K.; Mishima, K.; Srivastava, N.; Chandramohan, V.; Pegram, C.; Keir, S.T.; Kuan, C.T.; Bigner, D.D.; et al. Evaluation of anti-podoplanin rat monoclonal antibody NZ-1 for targeting malignant gliomas. *Nucl Med Biol* **2010**, *37*, 785-794, doi:10.1016/j.nucmedbio.2010.03.010.
54. Miura, K.; Yoshida, H.; Nosaki, S.; Kaneko, M.K.; Kato, Y. RAP Tag and PMab-2 Antibody: A Tagging System for Detecting and Purifying Proteins in Plant Cells. *Front Plant Sci* **2020**, *11*, 510444, doi:10.3389/fpls.2020.510444.
55. Fujii, Y.; Kaneko, M.K.; Ogasawara, S.; Yamada, S.; Yanaka, M.; Nakamura, T.; Saidoh, N.; Yoshida, K.; Honma, R.; Kato, Y. Development of RAP Tag, a Novel Tagging System for Protein Detection and Purification. *Monoclon Antib Immunodiagn Immunother* **2017**, *36*, 68-71, doi:10.1089/mab.2016.0052.
56. Fujii, Y.; Kaneko, M.K.; Kato, Y. MAP Tag: A Novel Tagging System for Protein Purification and Detection. *Monoclon Antib Immunodiagn Immunother* **2016**, *35*, 293-299, doi:10.1089/mab.2016.0039.

57. Wakasa, A.; Kaneko, M.K.; Kato, Y.; Takagi, J.; Arimori, T. Site-specific epitope insertion into recombinant proteins using the MAP tag system. *J Biochem* **2020**, *168*, 375-384, doi:10.1093/jb/mvaa054.
58. Mody, M.D.; Rocco, J.W.; Yom, S.S.; Haddad, R.I.; Saba, N.F. Head and neck cancer. *Lancet* **2021**, *398*, 2289-2299, doi:10.1016/s0140-6736(21)01550-6.
59. Ludwig, N.; Szczepanski, M.J.; Gluszko, A.; Szafarowski, T.; Azambuja, J.H.; Dolg, L.; Gellrich, N.C.; Kampmann, A.; Whiteside, T.L.; Zimmerer, R.M. CD44(+) tumor cells promote early angiogenesis in head and neck squamous cell carcinoma. *Cancer Lett* **2019**, *467*, 85-95, doi:10.1016/j.canlet.2019.10.010.
60. Boxberg, M.; Götz, C.; Haidari, S.; Dorfner, C.; Jesinghaus, M.; Drecoll, E.; Boskov, M.; Wolff, K.D.; Weichert, W.; Haller, B.; et al. Immunohistochemical expression of CD44 in oral squamous cell carcinoma in relation to histomorphological parameters and clinicopathological factors. *Histopathology* **2018**, *73*, 559-572, doi:10.1111/his.13496.
61. Chen, J.; Zhou, J.; Lu, J.; Xiong, H.; Shi, X.; Gong, L. Significance of CD44 expression in head and neck cancer: a systemic review and meta-analysis. *BMC Cancer* **2014**, *14*, 15, doi:10.1186/1471-2407-14-15.
62. de Jong, M.C.; Pramana, J.; van der Wal, J.E.; Lacko, M.; Peutz-Kootstra, C.J.; de Jong, J.M.; Takes, R.P.; Kaanders, J.H.; van der Laan, B.F.; Wachters, J.; et al. CD44 expression predicts local recurrence after radiotherapy in larynx cancer. *Clin Cancer Res* **2010**, *16*, 5329-5338, doi:10.1158/1078-0432.Ccr-10-0799.
63. Zöller, M. CD44: can a cancer-initiating cell profit from an abundantly expressed molecule? *Nat Rev Cancer* **2011**, *11*, 254-267, doi:10.1038/nrc3023.
64. Woerner, S.M.; Givehchian, M.; Dürst, M.; Schneider, A.; Costa, S.; Melsheimer, P.; Lacroix, J.; Zöller, M.; Doeberitz, M.K. Expression of CD44 splice variants in normal, dysplastic, and neoplastic cervical epithelium. *Clin Cancer Res* **1995**, *1*, 1125-1132.
65. Dall, P.; Heider, K.H.; Hekele, A.; von Minckwitz, G.; Kaufmann, M.; Ponta, H.; Herrlich, P. Surface protein expression and messenger RNA-splicing analysis of CD44 in uterine cervical cancer and normal cervical epithelium. *Cancer Res* **1994**, *54*, 3337-3341.
66. Dall, P.; Hekele, A.; Ikenberg, H.; Göppinger, A.; Bauknecht, T.; Pfleiderer, A.; Moll, J.; Hofmann, M.; Ponta, H.; Herrlich, P. Increasing incidence of CD44v7/8 epitope expression during uterine cervical carcinogenesis. *Int J Cancer* **1996**, *69*, 79-85, doi:10.1002/(sici)1097-0215(19960422)69:2<79::Aid-ijc2>3.0.Co;2-s.
67. Mereiter, S.; Martins Á, M.; Gomes, C.; Balmaña, M.; Macedo, J.A.; Polom, K.; Roviello, F.; Magalhães, A.; Reis, C.A. O-glycan truncation enhances cancer-related functions of CD44 in gastric cancer. *FEBS Lett* **2019**, *593*, 1675-1689, doi:10.1002/1873-3468.13432.
68. Rothenberg, S.M.; Ellisen, L.W. The molecular pathogenesis of head and neck squamous cell carcinoma. *J Clin Invest* **2012**, *122*, 1951-1957, doi:10.1172/jci59889.
69. Compagnone, M.; Gatti, V.; Presutti, D.; Ruberti, G.; Fierro, C.; Markert, E.K.; Vousden, K.H.; Zhou, H.; Mauriello, A.; Anemone, L.; et al. ΔNp63-mediated regulation of hyaluronic acid metabolism and signaling supports HNSCC tumorigenesis. *Proc Natl Acad Sci U S A* **2017**, *114*, 13254-13259, doi:10.1073/pnas.1711777114.
70. Stransky, N.; Egloff, A.M.; Tward, A.D.; Kostic, A.D.; Cibulskis, K.; Sivachenko, A.; Kryukov, G.V.; Lawrence, M.S.; Sougnez, C.; McKenna, A.; et al. The mutational landscape of head and neck squamous cell carcinoma. *Science* **2011**, *333*, 1157-1160, doi:10.1126/science.1208130.
71. Menke-van der Houven van Oordt, C.W.; Gomez-Roca, C.; van Herpen, C.; Coveler, A.L.; Mahalingam, D.; Verheul, H.M.; van der Graaf, W.T.; Christen, R.; Rüttinger, D.; Weigand, S.; et al. First-in-human phase I clinical trial of RG7356, an anti-CD44 humanized antibody, in patients with advanced, CD44-expressing solid tumors. *Oncotarget* **2016**, *7*, 80046-80058, doi:10.18632/oncotarget.11098.
72. Riechelmann, H.; Sauter, A.; Golze, W.; Hanft, G.; Schroen, C.; Hoermann, K.; Erhardt, T.; Gronau, S. Phase I trial with the CD44v6-targeting immunoconjugate bivatuzumab mertansine in head and neck squamous cell carcinoma. *Oral Oncol* **2008**, *44*, 823-829, doi:10.1016/j.oraloncology.2007.10.009.
73. Tijink, B.M.; Buter, J.; de Bree, R.; Giaccone, G.; Lang, M.S.; Staab, A.; Leemans, C.R.; van Dongen, G.A. A phase I dose escalation study with anti-CD44v6 bivatuzumab mertansine in patients with incurable squamous cell carcinoma of the head and neck or esophagus. *Clin Cancer Res* **2006**, *12*, 6064-6072, doi:10.1158/1078-0432.Ccr-06-0910.
74. Mitsunaga, M.; Ogawa, M.; Kosaka, N.; Rosenblum, L.T.; Choyke, P.L.; Kobayashi, H. Cancer cell-selective in vivo near infrared photoimmunotherapy targeting specific membrane molecules. *Nat Med* **2011**, *17*, 1685-1691, doi:10.1038/nm.2554.
75. Maruoka, Y.; Wakiyama, H.; Choyke, P.L.; Kobayashi, H. Near infrared photoimmunotherapy for cancers: A translational perspective. *EBioMedicine* **2021**, *70*, 103501, doi:10.1016/j.ebiom.2021.103501.
76. Kato, T.; Wakiyama, H.; Furusawa, A.; Choyke, P.L.; Kobayashi, H. Near Infrared Photoimmunotherapy; A Review of Targets for Cancer Therapy. *Cancers (Basel)* **2021**, *13*, doi:10.3390/cancers13112535.
77. Ogawa, M.; Tomita, Y.; Nakamura, Y.; Lee, M.J.; Lee, S.; Tomita, S.; Nagaya, T.; Sato, K.; Yamauchi, T.; Iwai, H.; et al. Immunogenic cancer cell death selectively induced by near infrared photoimmunotherapy initiates host tumor immunity. *Oncotarget* **2017**, *8*, 10425-10436, doi:10.18632/oncotarget.14425.

78. Cognetti, D.M.; Johnson, J.M.; Curry, J.M.; Kochuparambil, S.T.; McDonald, D.; Mott, F.; Fidler, M.J.; Stenson, K.; Vasan, N.R.; Razaq, M.A.; et al. Phase 1/2a, open-label, multicenter study of RM-1929 photoimmunotherapy in patients with locoregional, recurrent head and neck squamous cell carcinoma. *Head Neck* **2021**, *43*, 3875-3887, doi:10.1002/hed.26885.
79. Nagaya, T.; Nakamura, Y.; Okuyama, S.; Ogata, F.; Maruoka, Y.; Choyke, P.L.; Allen, C.; Kobayashi, H. Syngeneic Mouse Models of Oral Cancer Are Effectively Targeted by Anti-CD44-Based NIR-PIT. *Mol Cancer Res* **2017**, *15*, 1667-1677, doi:10.1158/1541-7786.Mcr-17-0333.
80. Li, G.; Suzuki, H.; Ohishi, T.; Asano, T.; Tanaka, T.; Yanaka, M.; Nakamura, T.; Yoshikawa, T.; Kawada, M.; Kaneko, M.K.; et al. Antitumor activities of a defucosylated anti-EpCAM monoclonal antibody in colorectal carcinoma xenograft models. *Int J Mol Med* **2023**, *51*, doi:10.3892/ijmm.2023.5221.
81. Nanamiya, R.; Takei, J.; Ohishi, T.; Asano, T.; Tanaka, T.; Sano, M.; Nakamura, T.; Yanaka, M.; Handa, S.; Tateyama, N.; et al. Defucosylated Anti-Epidermal Growth Factor Receptor Monoclonal Antibody (134-mG(2a)-f) Exerts Antitumor Activities in Mouse Xenograft Models of Canine Osteosarcoma. *Monoclon Antib Immunodiagn Immunother* **2022**, *41*, 1-7, doi:10.1089/mab.2021.0036.
82. Kawabata, H.; Suzuki, H.; Ohishi, T.; Kawada, M.; Kaneko, M.K.; Kato, Y. A Defucosylated Mouse Anti-CD10 Monoclonal Antibody (31-mG(2a)-f) Exerts Antitumor Activity in a Mouse Xenograft Model of CD10-Overexpressed Tumors. *Monoclon Antib Immunodiagn Immunother* **2022**, *41*, 59-66, doi:10.1089/mab.2021.0048.
83. Kawabata, H.; Ohishi, T.; Suzuki, H.; Asano, T.; Kawada, M.; Suzuki, H.; Kaneko, M.K.; Kato, Y. A Defucosylated Mouse Anti-CD10 Monoclonal Antibody (31-mG(2a)-f) Exerts Antitumor Activity in a Mouse Xenograft Model of Renal Cell Cancers. *Monoclon Antib Immunodiagn Immunother* **2022**, doi:10.1089/mab.2021.0049.
84. Asano, T.; Tanaka, T.; Suzuki, H.; Li, G.; Ohishi, T.; Kawada, M.; Yoshikawa, T.; Kaneko, M.K.; Kato, Y. A Defucosylated Anti-EpCAM Monoclonal Antibody (EpMab-37-mG(2a)-f) Exerts Antitumor Activity in Xenograft Model. *Antibodies (Basel)* **2022**, *11*, doi:10.3390/antib11040074.
85. Tateyama, N.; Nanamiya, R.; Ohishi, T.; Takei, J.; Nakamura, T.; Yanaka, M.; Hosono, H.; Saito, M.; Asano, T.; Tanaka, T.; et al. Defucosylated Anti-Epidermal Growth Factor Receptor Monoclonal Antibody 134-mG(2a)-f Exerts Antitumor Activities in Mouse Xenograft Models of Dog Epidermal Growth Factor Receptor-Overexpressed Cells. *Monoclon Antib Immunodiagn Immunother* **2021**, *40*, 177-183, doi:10.1089/mab.2021.0022.
86. Takei, J.; Ohishi, T.; Kaneko, M.K.; Harada, H.; Kawada, M.; Kato, Y. A defucosylated anti-PD-L1 monoclonal antibody 13-mG(2a)-f exerts antitumor effects in mouse xenograft models of oral squamous cell carcinoma. *Biochem Biophys Rep* **2020**, *24*, 100801, doi:10.1016/j.bbrep.2020.100801.